Journal of Power Sources 186 (2009) 565–569

Contents lists available at ScienceDirect

Journal of Power Sources

journal homepage: www.elsevier.com/locate/jpowsour

Short communication

Electrochemical supercapacitor behavior of $Ni_3(Fe(CN)_6)_2(H_2O)$ nanoparticles

Jie Chen, Kelong Huang*, Suqin Liu, Xi Hu

College of Chemistry and Chemical Engineering, Central South University, Changsha, Hunan 410083, China

ARTICLE INFO

Article history:
Received 2 June 2008
Received in revised form 8 August 2008
Accepted 12 August 2008
Available online 2 September 2008

Keywords:
Supercapacitor
$Ni_3(Fe(CN)_6)_2(H_2O)$
Nanoparticles

ABSTRACT

Nanosized $Ni_3(Fe(CN)_6)_2(H_2O)$ was prepared by a simple co-precipitation method. The electrochemical properties of the sample as the electrode material for supercapacitor were studied by cyclic voltammetry (CV), constant charge/discharge tests and electrochemical impedance spectroscopy (EIS). A specific capacitance of 574.7 F g^{-1} was obtained at the current density of 0.2 A g^{-1} in the potential range from 0.3 V to 0.6 V in 1 M KNO_3 electrolyte. Approximately 87.46% of specific discharge capacitance was remained at the current density of 1.4 A g^{-1} after 1000 cycles.

1. Introduction

Transition metal hexacyanoferrates of the general formula $A_hM_k[Fe(CN)_6]_l$ (where *h*, *k*, and *l* are stoichiometric numbers, A = alkali metal cation, M = transition metal) represent an important class of mixed-valence compounds, of which Prussian blue is the classical prototype [1]. Aside from their interesting solid-state chemistry and structural attributes, these compounds exhibit interesting magnetic, optical, and electrochemical properties and thus have great potential for device applications (e.g. molecular magnets, electrodes and rechargeable batteries) [2–6]. PB and its analogues have open spaces due to the large asymmetric CN^- anion, and they connect with each other to form a tunnel structure, which can accommodate not only neutral molecules but also ions charge-balanced by the iron ions [7]. Besides, they are non-toxic compounds whose redox reactions are chemically reversible. Thus, these materials have raised renewed and growing interest in the electrochemical field.

Among the electrode materials for application in supercapacitors, amorphous $RuO_2{\cdot}xH_2O$ was reported as the most promising electrode material for supercapacitor with a specific capacitance of 720 F g^{-1} [8]. But the high cost and environmental toxicity of this material limit its extensive use in commercial applications. Efforts have been made to find a cheap and environmental friendly material with good electrochemical performance to replace RuO_2. Lisowaka-Oleksiak et al. [9] prepared metal hexacyanoferrate network inside polymer matrix for electrochemical capacitors by the electrochemical deposition process, showing higher capacitance of the hybrid films due to presence of inorganic networks. But the preparation of these hybrid films was relatively complicated. In this work, an insoluble transition metal hexacyanoferrates $Ni_3(Fe(CN)_6)_2(H_2O)$ was prepared by a simple co-precipitation method. Furthermore, cyclic voltammogram (CV), constant charge/discharge and electrochemical impedance spectroscopy were employed to assess the potential application of the as-prepared material as the active electrode material of supercapacitor in 1 M KNO_3 solution.

2. Experimental

All reagents used in this experiment were of analytical grade without further purification. A typical experiment procedure was as follows: $Ni_3(Fe(CN)_6)_2(H_2O)$ was synthesized by adding (100 ml, 0.1 M) $K_3[Fe(CN)_6]$ into (100 ml, 0.1 M) $Ni(NO_3)_2{\cdot}6H_2O$ slowly. The mixture was stirred for 30 min under room temperature. When finished, the brown precipitates were centrifuged, filtered, and washed with deionized water for several times, and finally dried at 80 °C for 8 h. The formation of insoluble precipitate was a driving force of the observed changes.

X-ray powder diffraction data was collected on a Rigaku D/max2550VB$^+$18kw with Cu Kα radiation, scan range from 10° to 90°. The morphology of as-prepared particles was characterized a JE01-1230 transmission electron microscope.

The $Ni_3(Fe(CN)_6)_2(H_2O)$ electrode was prepared by mixing 75 wt.% $Ni_3(Fe(CN)_6)_2(H_2O)$ powders, 20 wt.% acetylene black and 5 wt.% PTFE binder. The mixture was pressed onto stainless steel grids, which serves as current collector, and then dried at

* Corresponding author. Tel.: +86 731 8830827; fax: +86 731 8879850.
E-mail address: klhuang@mail.csu.edu.cn (K. Huang).

0378-7753/$ – see front matter © 2008 Published by Elsevier B.V.
doi:10.1016/j.jpowsour.2008.08.071

100 °C under vacuum for 12 h. The electrochemical behavior of $Ni_3(Fe(CN)_6)_2(H_2O)$ was characterized by cyclic voltammetry (CV), electrochemical impedance spectroscopy and charge/discharge tests. The experiments were carried out in a conventional three-electrode electrochemical cell. The prepared $Ni_3(Fe(CN)_6)_2(H_2O)$ electrode was used as the working electrode, a saturated calomel electrode (SCE) was used as the reference electrode and a platinum foil of convenient area was set as the counter electrode. The electrolytes in this experiment consisted of 1 M KNO_3, $LiNO_3$ and $NaNO_3$ solution. CV and constant charge/discharge tests were performed using a CHI660 workstation (Shanghai, China). Electrochemical impedance spectroscopy was performed by ZAHNER-IM6 electrochemical workstation (Germany). The impedance spectra were recorded by applying an AC voltage of 5 mV amplitude in the frequency range from 0.01 Hz to 1 MHz.

3. Results and discussion

3.1. Material characteristics

The crystal structure was determined by X-ray diffraction (XRD) measurements. Fig. 1 presents the typical diffraction pattern of the product. All the peaks of Fig. 1 can be indexed as cubic nickel iron cyanide hydrate $Ni_3(Fe(CN)_6)_2(H_2O)$ (space group F-43m) with a lattice parameter of 10.23 Å, which was in good agreement with the values from the standard card (JCPDS no. 82-2283).

The morphology of the as-prepared sample was investigated by TEM. As shown in Fig. 2, the sample consisted of a large quantity of particles with a size of around 20 nm.

3.2. Electrochemical analysis

Cyclic voltammeric curves of the $Ni_3(Fe(CN)_6)_2(H_2O)$ electrode in 1 M KNO_3, 1 M $LiNO_3$ and 1 M $NaNO_3$ solution at the potential scanning rate of 5 mV s^{-1} in the potential range from 0 V to 1 V are presented in Fig. 3. As shown in Fig. 3, $Ni_3(Fe(CN)_6)_2(H_2O)$ electrode showed stronger current response and higher specific capacitance in 1 M KNO_3 solution than in 1 M $NaNO_3$ or 1 M $LiNO_3$ solution, which may result from the different hydrated radiuses of K^+, Li^+ and Na^+. PB and its analogues have open spaces due to the large asymmetric CN^- anion, they connect each other to form a tunnel structure, which can accommodate not only neutral molecules but also ions charge-balanced by the iron ions [7]. But the sizes of hydrated ions have great influence with the ability of the various ions to reversibly enter the structure [10]. The radius of hydrated K^+ (1.28 Å) was the smallest one among these three cations (K^+, Li^+ and Na^+) [11], which resulted in the fast insertion/extraction kinetics of K^+ in $Ni_3(Fe(CN)_6)_2(H_2O)$ electrode.

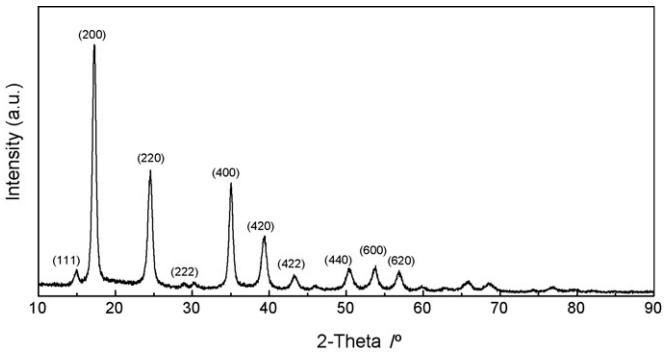

Fig. 1. XRD patterns of the as-prepared particles.

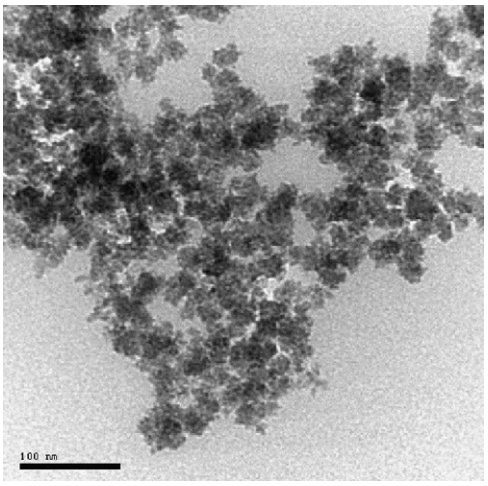

Fig. 2. TEM images of the as-prepared particles.

The cyclic voltammograms of $Ni_3(Fe(CN)_6)_2(H_2O)$ electrode in 1 M KNO_3 solution at different voltage scan rates (5, 10, 15, 20, and 25 mV s^{-1})in the potential range of 0–1 V are shown in Fig. 4(a). The shape of the curves revealed that the capacitance characteristics were very distinguished from that of electric double-layer capacitance in which the shape is normally close to an ideal rectangular shape, indicating that the capacity mainly resulted from the pseudocapacitive capacitance, which was caused by the fast and reversible faradaic redox reactions of electroactive material. It is known for the work of Kulesza et al. [12] that nickel hexacyanoferrate in aqueous electrolytes may show activity of low-spin iron ion redox center only [11]. Nickel atoms in $Ni_3(Fe(CN)_6)_2(H_2O)$ are known to be at valence state (II). Thus, The couple of redox peaks observed within the potential range in 1 M KNO_3 solution may be related to the iron (II/III) couple coordinated by cyanide groups via carbon atoms (low spin complex) [13], which may be ascribed to the reaction below:

$$Ni_{1.5}^{II}[Fe^{III}(CN)_6] + K^+ + e^- \rightarrow KNi_{1.5}^{II}[Fe^{II}(CN)_6]$$

As shown in Fig. 4(a), the redox peak profiles were symmetric, indicating the good reversibility of the electrochemical reaction that took place on the $Ni_3(Fe(CN)_6)_2(H_2O)$ electrode. As the potential scanning rates increased, the voltage difference between the

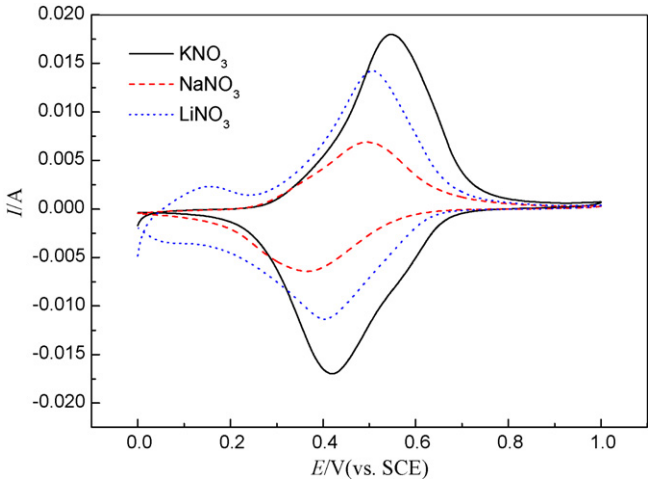

Fig. 3. Cyclic voltammograms of $Ni_3(Fe(CN)_6)_2(H_2O)$ electrode in different electrolytes.

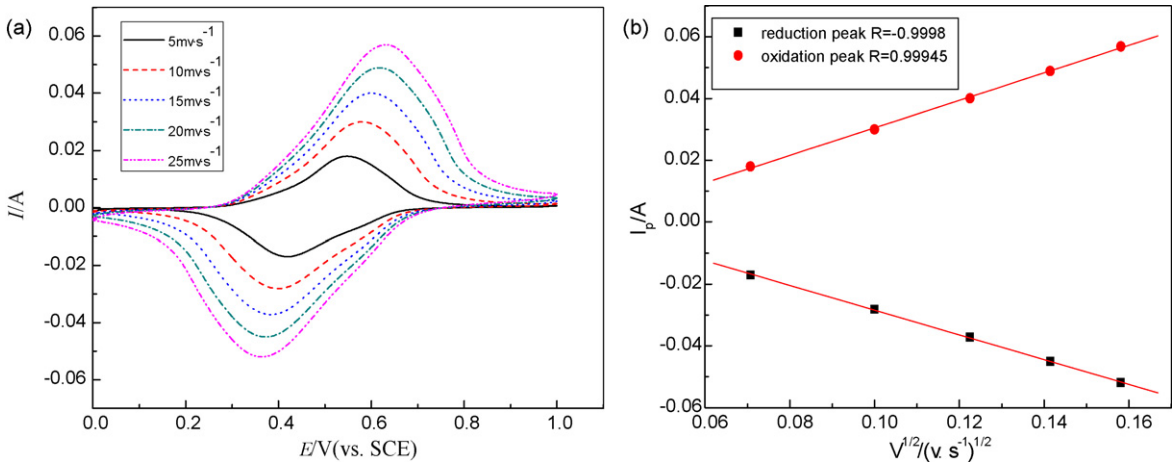

Fig. 4. Cyclic voltammograms of $Ni_3(Fe(CN)_6)_2(H_2O)$ electrode in 1 M KNO_3 at various scan rates (a). The relationship between the peak current (i_p) and the square root of the scan rate ($\upsilon^{1/2}$) of the redox pairs (b).

oxidation and reduction peak also increased due to the polarization of electrode under high potential scanning rate. Besides, the peak current (i_p) changed with the increase of potential scanning rate, indicating the fast redox process on the electrode. The diffusion equation gives a relationship between peak current (i_p) and the square root of the scan rate ($\upsilon^{1/2}$), as shown below [14]:

$$i_p = 2.69 \times 10^5 An^{3/2} C_0 D^{1/2} \nu^{1/2}$$

where n is the number of electrons per molecule during the intercalation, A is the surface area of the electrode, C_0 is the concentration of diffusion species (K^+), D is the diffusion coefficient of K^+ and ν is the potential scanning rate. According to the equation above, the relationship between the peak current (i_p) and the square root of the scan rate ($\upsilon^{1/2}$) of the redox pairs was shown in Fig. 4(b). As shown in this figure, a good linear relationship between i_p and $\upsilon^{1/2}$ was observed, indicating that the reaction kinetics was controlled by the diffusion process of hydrated potassium cations in solution.

In order to obtain information about the ability of $Ni_3(Fe(CN)_6)_2(H_2O)$ as electrode material in supercapacitor, constant current charge/discharge measurement was carried out in 1 M KNO_3. Fig. 5(a) shows the constant current charge/discharge curve of the $Ni_3(Fe(CN)_6)_2(H_2O)$ electrode at the current density of 0.2 A g^{-1} in the potential range from 0.3 V to 0.6 V. During the charge and discharge steps, the curve obviously displayed two variation range, a linear variation of the time dependence of the potential (below about 0.4 V) indicate pure double-layer capacitance behavior, which was caused by the charge separation taking place between the electrode and electrolyte interface [15], and a slope variation of the time dependence of the potential (0.4–0.6 V) indicate a typical pseudo-capacitance behavior, which may result from the electrochemical redox reaction at an interface between electrode and electrolyte. The discharge-specific capacitance (C_m) of this electrode could be calculated from the discharge curves, as shown below:

$$C_m = \frac{i\,\Delta t}{m\,\Delta V} \tag{2}$$

where i is the discharge current (A), Δt is the total discharge time (s), m is the mass of the $Ni_3(Fe(CN)_6)_2(H_2O)$ electrode (g), ΔV is the potential drop during discharge. According to Eq. (2), the discharge-specific capacitance of the electrode at the current density of 0.2 A g^{-1} was 574.7 F g^{-1}. The coulombic efficiency was around 98%. The relationship between the current density and the discharge-specific capacitance was shown in Fig. 5(b). As shown in Fig. 5(b), when the current density was increased to 1.8 A g^{-1}, the specific discharge capacitance remained 453.5 F g^{-1}. The specific capacitance only slightly decreased with the increase of current

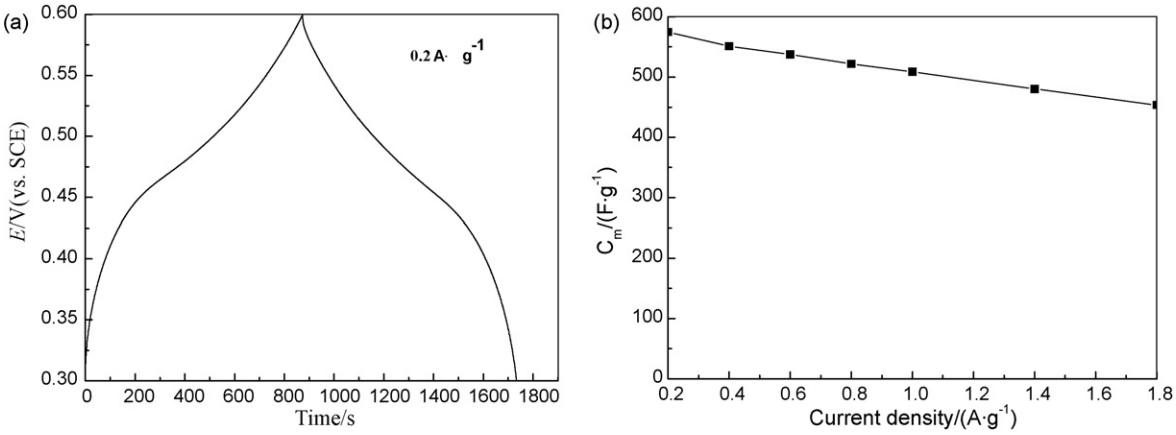

Fig. 5. Constant charge/discharge curve of the $Ni_3(Fe(CN)_6)_2(H_2O)$ electrode in 1 M KNO_3 under the current density of 0.2 A g^{-1} (a) and the relationship of the current density with the discharge-specific capacitance (b).

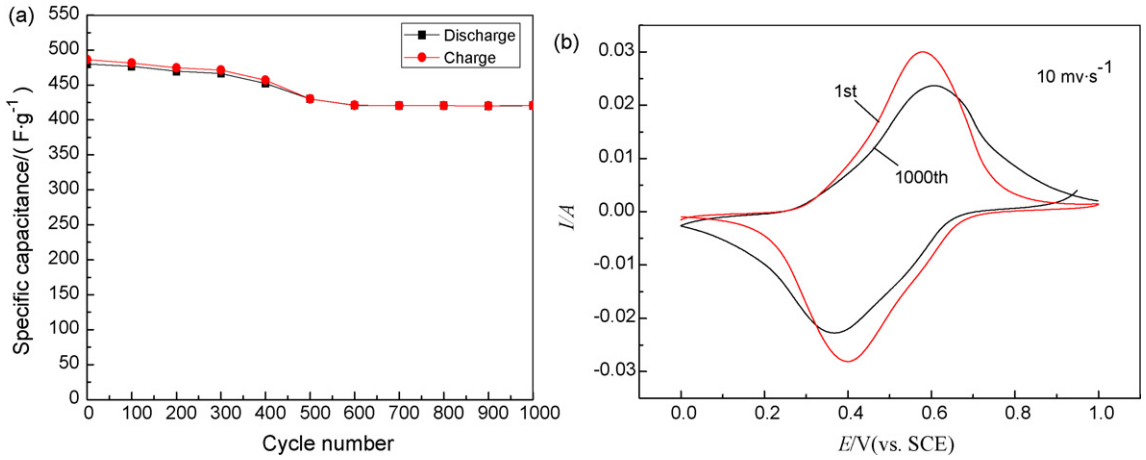

Fig. 6. (a) Cycling performance of the $Ni_3(Fe(CN)_6)_2(H_2O)$ electrode at the current density of 1.4 A g^{-1} in 1 M KNO_3 and (b) cyclic voltammograms of the $Ni_3(Fe(CN)_6)_2(H_2O)$ electrode under different cycle numbers.

density, indicating that the $Ni_3(Fe(CN)_6)_2(H_2O)$ electrode could charge/discharge under high current density. But the potential window of this electrode was narrower than that of RuO_2.

The cycle charge/discharge test has been employed to examine the service life of the $Ni_3(Fe(CN)_6)_2(H_2O)$ material. The variation of specific capacitance as a function of cycle number at the current density of 1.4 A g^{-1} was shown in Fig. 6. As shown in this figure, approximately 87.46% of specific discharge-specific capacitance was remained after 1000 cycles under high current density. The coulombic efficiency was around 99% for all cycles. Fig. 6(b) shows the cyclic voltammograms of the $Ni_3(Fe(CN)_6)_2(H_2O)$ electrode at the 1st cycle and 1000th cycle at the potential scanning rate of 10 mV s^{-1}. The cyclic voltammograms under different cycle numbers were of the same shape, indicating the good reversibility of the electrochemical reaction on the $Ni_3(Fe(CN)_6)_2(H_2O)$ electrode. But the area of the CV curves reduced slightly, indicating the slight attenuation of capacitance of the electrode, which was in consistence with the result of Fig. 6(a). As discussed above, the $Ni_3(Fe(CN)_6)_2(H_2O)$ electrode exhibited good capacity retention and capacitive property, indicating that the $Ni_3(Fe(CN)_6)_2(H_2O)$ material had the potential of being used as the electrode material of supercapacitor.

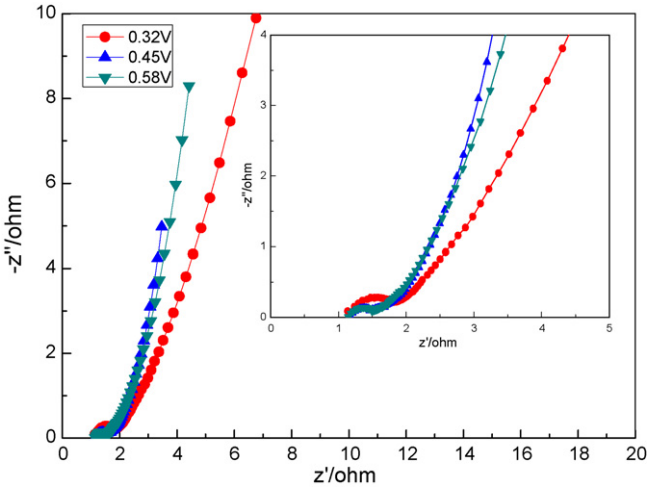

Fig. 7. Typical electrochemical impedance spectroscopy of the electrode at different applied potentials.

Electrochemical impedance spectroscopy (EIS) for the $Ni_3(Fe(CN)_6)_2(H_2O)$ electrode were carried out at different potentials (at applied potential of 0.32 V, 0.45 V and 0.58 V; the frequency range is 0.01 Hz–1 MHz) of interest over the capacitor operating potential range, which are shown in Fig. 7. As shown in this figure, the impedance spectra under different potentials were composed of three regions. In the low-frequency region, the impedance slope of straight line was more vertical as the testing potential increased. The straight line in low-frequency range is inclined at the angle of approximately 90° to the real axis, indicating that the $Ni_3(Fe(CN)_6)_2(H_2O)$ electrode had a good capacitive behavior in 1 M KNO_3 solution [14]. In the intermediate frequency is the 45° line that is the characteristic of ion diffusion into the electrode materials. From the point intersecting with the real axis in the range of high frequency, the solution resistance of these systems was about 1 Ω, and the resistance of the $Ni_3(Fe(CN)_6)_2(H_2O)$ electrode was around 0.5 Ω. As discussed above, the $Ni_3(Fe(CN)_6)_2(H_2O)$ electrode had a good capacitive behavior in 1 M KNO_3 within certain potential window (from 0.32 V to 0.58 V), which was consistent with the results of CV test and constant charge/discharge test.

4. Conclusion

Nanosized $Ni_3(Fe(CN)_6)_2(H_2O)$ was prepared by a simple co-precipitation method using only $K_3[Fe(CN)_6]$ and $Ni(NO_3)_2{\cdot}6H_2O$ as the raw materials. The potential of utilizing this material as electrode active material for supercapacitor was examined by CV, constant charge/discharge and electrochemical impedance spectroscopy. The results showed that the $Ni_3(Fe(CN)_6)_2(H_2O)$ material exhibited higher specific capacitance in 1 M KNO_3 than in $NaNO_3$ or $LiNO_3$ solution within the potential range from 0 V to 1 V, which may result from the different hydrated radiuses of K^+, Li^+ and Na^+. The discharge-specific capacitance of the $Ni_3(Fe(CN)_6)_2(H_2O)$ electrode in 1 M KNO_3 was 574.7 F g^{-1} at the current density of 0.2 A g^{-1} in the potential range from 0.3 V to 0.6 V. As the current density increased to 1.8 A g^{-1}, the discharge-specific capacitance of the electrode was 453.5 F g^{-1}, indicating that the $Ni_3(Fe(CN)_6)_2(H_2O)$ electrode could charge/discharge at high current density. After 1000 cycles, approximately 87.46% of discharge-specific capacitance was remained at the current density of 1.4 A g^{-1}. The $Ni_3(Fe(CN)_6)_2(H_2O)$ electrode exhibited good capacity retention and capacitive property. Thus, the $Ni_3(Fe(CN)_6)_2(H_2O)$ material had the potential of being used as the electrode material of supercapacitor.

Acknowledgements

We wish to thank the Natural Science Foundation of China (No. E50772133) and Innovation Projects for Graduates of Center South University (No. 1343-74335000009) for its financial support of this project.

References

[1] K.R. Dunbar, R.A. Heintz, Prog. Inorg. Chem. 45 (1997) 283.
[2] K. Itaya, I. Uchida, V.D. Neff, Acc. Chem. Res. 19 (1986) 162.
[3] N.R. Tacconi, K. Rajeshwar, R.O. Lezna, Chem. Mater. 15 (2003) 3046.
[4] K. Aoki, T. Miyamoto, Y. Ohsawa, Bull. Chem. Chem. Soc. Jpn. 62 (1989) 1658.
[5] N. Imanishi, T. Morikawa, J. Kondo, Y. Takeda, O. Yamamoto, N. Kinugasa, T. Yamagishi, J. Power Sources 79 (1999) 215–219.
[6] A. Burke, J. Power Sources 91 (2000) 37.
[7] J.F. Keggin, F.D. Miles, Nature 137 (1936) 577.
[8] J.P. Zheng, T.R. Jow, J. Electrochem. Soc. 144 (1997) 2026.
[9] A. Lisowska-Oleksiak, A.P. Nowak., J. Power Sources 173 (2007) 829–836.
[10] R.A. Huggins, Solid State Ionics 113–115 (1998) 533–544.
[11] K. Itaya, T. Ataka, S. Toshima, J. Am. Chem. Soc. 104 (1982) 4767.
[12] P.J. Kulesza, S. Zamponi, M.A. Malik, M. Berrettoni, A. Wolkiewicz, R. Marassi, Electrochim. Acta 48 (2003) 4261–4269.
[13] M.A. Malik, K. Miecznikowski, P.J. Kulesza, Electrochim. Acta 45 (2000) 3777.
[14] A.J. Bard, L.R. Faulkner, Electrochemical Methods, John Wiley & Sons, Inc., New York, 1980.
[15] W. Sugimoto, H. Iwata, Y. Yasunaga, Y. Murakami, Y. Takasu, Angew. Chem. Int. Ed. 42 (2003) 4092.